THE JOURNAL OF BIOLOGICAL CHEMISTRY
Vol. 277, No. 40, Issue of October 4, pp. 37863–37870, 2002
© 2002 by The American Society for Biochemistry and Molecular Biology, Inc.
Printed in U.S.A.

Prothrombinase Assembly and S1 Site Occupation Restore the Catalytic Activity of FXa Impaired by Mutation at the Sodium-binding Site*

Received for publication, April 16, 2002, and in revised form, June 21, 2002
Published, JBC Papers in Press, July 30, 2002, DOI 10.1074/jbc.M203692200

Rodney M. Camire‡

From the Joseph Stokes, Jr. Research Institute, Division of Hematology, The Children's Hospital of Philadelphia, Philadelphia, Pennsylvania 19104

Two loop segments (183–189 and 221–225) in the protease domain of factor Xa contribute to the formation of a Na^+-binding site. Studies with factor Xa indicate that binding of a single Na^+ ion to this site influences its activity by altering the S1 specificity site, and substitution of Tyr^{225} with Pro diminishes sensitivity to Na^+. Using full-length factor Xa^{Y225P}, the allosteric relationship between the Na^+ site and other structural determinants in factor Xa and prothrombinase was investigated. Direct binding and kinetic measurements with probes that target the S1 specificity pocket indicate that assembly of the mutant in prothrombinase corrected the impaired binding of these probes observed with free factor Xa^{Y225P}. This appears to result from the apparent allosteric linkage between the factor Va, S1, and Na^+-binding sites, since binding of the cofactor to membrane-bound factor Xa^{Y225P} enhances binding at the S1 site and *vice versa*. Additional studies revealed that the internal salt bridge (Ile^{16}–Asp^{194}) of factor Xa^{Y225P} is partially destabilized, a process that is reversible upon occupation of the S1 site. The data establish that alterations at the factor Xa Na^+-binding site shift the zymogen-protease equilibrium to a more zymogen-like state, and as a consequence binding of S1-directed probes and factor Va are adversely affected. Therefore, the zymogen-like characteristics of factor Xa^{Y225P} have allowed for the apparent allosteric linkage between the S1, factor Va, and Na^+ sites to become evident and has provided insight into the structural transitions which accompany the conversion of factor X to factor Xa.

Factor X (FX)[1] is a vitamin K-dependent two-chain glycoprotein that plays a central role in blood coagulation. This serine protease zymogen is a substrate for both the extrinsic (tissue factor/FVIIa) and intrinsic (FVIIIa/FIXa) tenase enzyme complexes, which cleave the Arg^{15}–Ile^{16} scissile bond[2] in FX, releasing a 52-amino acid activation peptide generating FXa (1). Factor Xa reversibly associates with its cofactor FVa on a membrane surface in the presence of Ca^{2+} ions to form prothrombinase (2). While FXa catalyzes prothrombin cleavage, the macromolecular interactions that stabilize prothrombinase lead to a profound enhancement in catalytic efficiency (2), indicating that prothrombinase, not FXa, is the physiologically relevant enzyme leading to explosive thrombin generation.

Several studies have established that small ligands such as Na^+ and Ca^{2+} can allosterically modulate the protease domain function of FXa (3–9). Orthner and Kosow (4) demonstrated that FXa is capable of discriminating among monovalent and divalent cations, and both Na^+ and Ca^{2+} were found to stimulate the cleavage of oligopeptidyl substrates. The location of the Na^+- and Ca^{2+}-binding sites in the protease domain has been identified through structural studies (10, 11). The Ca^{2+} site in the protease domain is essentially the same as that of trypsin (12), consisting of the Asp^{70}–Glu^{80} loop. Whereas Na^+ occupies a similar site in FXa as compared with thrombin, the coordinating ligands to Na^+ differ, employing two loop segments (183–189 and 221–225; residues that are part of the so-called activation domain of serine proteases), involving four carbonyl oxygen atoms and two water molecules (11).

It has become apparent over the past several years that metal ion binding sites in the catalytic domain of several serine proteases are allosterically linked to various structural determinants (8, 13–17). For example, two recent studies have shown that the Ca^{2+}- and Na^+-binding sites in FXa appear to be allosterically linked (*e.g.* changes at one site influence the other and *vice versa*) (9, 18). In addition to linkage between the Na^+- and Ca^{2+}-binding sites, the S1 specificity site is also allosterically linked to the Na^+-binding site but not the Ca^{2+} site (9). Similar results were also recently reported for the anticoagulant protein, activated protein C (19).

Whether Na^+ binding to the catalytic domain of serine proteases has physiological relevance is open to debate, considering that the plasma concentration of Na^+ is tightly regulated at ~150 mM. It is important to consider, however, that for certain enzymes such as thrombin, the dissociation constant for Na^+ is close to 150 mM (13), indicating that small changes in the cation concentration or, more likely, changes in the availability of allosteric effector molecules that are linked to the Na^+-binding site can dramatically influence enzyme activity (20). The re-

* This work was supported by National Institutes of Health Grant NRSA HL10343-02. Part of this work was presented in abstract form at the 42nd Annual Meeting of the American Society of Hematology, December 1–5, 2000, San Francisco, CA (70). The costs of publication of this article were defrayed in part by the payment of page charges. This article must therefore be hereby marked "*advertisement*" in accordance with 18 U.S.C. Section 1734 solely to indicate this fact.

‡ To whom correspondence may be addressed: Division of Hematology, 310B Abramson Research Center, The Children's Hospital of Philadelphia, 34th St. and Civic Center Blvd., Philadelphia, PA 19104. Tel.: 215-590-9968; Fax: 215-590-3660; E-mail: camire@email.chop.edu.

[1] The abbreviations used are: FX, factor X; FXa, activated FX; FV, factor V; FVa, activated FV; FIX, factor IX; FVII, factor VII; pdFX, plasma-derived FX; rFX, recombinant FX; pdFXa, plasma-derived FXa; rwtFXa, recombinant wild-type FXa; $RVV_{X\text{-}CP}$, FX activator from Russell's viper venom; PAB, 4-aminobenazmidine; SpecXa, methoxycarbonyl-cyclohexylglycyl-glycyl-arginine-*p*-nitroanilide; HEK 293, human embryonic kidney cells; rTAP, recombinant tick anticoagulant peptide; PCPS, small unilamellar vesicles composed of 75% (w/w) phosphatidylcholine and 25% (w/w) phosphatidylserine; Gla, 4-carboxyglutamic acid; MES, 4-morpholineethanesulfonic acid; S-2222, benzoyl isoleucyl-glutamyl-glycinyl-arginyl-*p*-nitroanilide; S-2765, *N*-α-benzyloxycarbonyl-arginyl-glycyl-arginine-*p*-nitroanilide; IEGR-AMC, isoleucyl-glutamyl-glycyl-arginine 7-amido-4-methylcoumarin; PTH, phenylthiohydantoin.

[2] Residue numbers in FX are based upon the chymotrypsinogen numbering system (69).

ported dissociation constant of Na^+ for calcium-bound APC is ~23 mM, indicating that *in vivo* most of the APC would be bound to Na^+ (19). The results with FXa and prothrombinase, however, are less clear. For example, the reported dissociation constant of Na^+ for calcium-bound FXa ranges from 43 to 280 mM (9, 18, 21). Results with prothrombinase indicate that the activity of wild-type FXa incorporated into prothrombinase using various monovalent cations was minimally (<1.5-fold) affected by the presence of Na^+ in the reaction buffer. However, this apparently was not the case using a Gla domainless form of FXa incorporated into prothrombinase or a Gla domainless variant ($GDFXa^{Y225P}$), since the rate of prethrombin-1 activation in the absence of Na^+ was dramatically decreased (18). The Tyr^{225} to Pro variant in GDFXa and thrombin was shown to be essentially insensitive to Na^+, and it behaves in a similar fashion to the wild-type enzymes assayed in the absence of Na^+ (15, 18, 22). Reasons for the discrepancy between $GDFXa^{Y225P}$ and GDFXa incorporated into prothrombinase in the absence of Na^+ compared with full-length FXa are currently not clear, but they could relate to unanticipated effects of various monovalent cations on other constituents of prothrombinase or to the nature of GDFXa compared with full-length FXa in the assembly and function within prothrombinase under these conditions.

In the current study, three unresolved questions with respect to the FXa Na^+-binding site were investigated: 1) does alteration of the Na^+-binding site affect prothrombinase complex assembly; 2) what is the molecular basis for the reduced affinity of active site-directed probes for FXa in the absence of Na^+; and 3) is the FXa Na^+ binding site allosterically linked to other structural determinants in the protease domain? These questions were approached using a full-length, fully γ-carboxylated derivative of FXa, $rFXa^{Y225P}$. This particular variant of FXa is a useful tool to study the Na^+-free state of the enzyme, since it has a markedly reduced sensitivity toward Na^+ (as does thrombin Y225P (22)), thus allowing for assessment of prothrombinase assembly in the presence of physiologically relevant concentrations of this monovalent cation.

EXPERIMENTAL PROCEDURES

Materials—Hepes, sodium chloride, sodium cyanate, and polyethylene glycol (average M_r = 8000) were from J. T. Baker Inc. Coomassie Brilliant Blue R-250, calcium chloride, EDTA, Russell's viper venom, and IEGR-AMC were purchased from Sigma. The fluorophore 4-aminobenazmidine (PAB) was from Aldrich. The concentrations of IEGR-AMC and PAB were determined in water using E_{325} = 17,200 M^{-1} cm^{-1} (23) and E_{293} = 15,000 M^{-1} cm^{-1} (24), respectively. The peptidyl substrate methoxycarbonyl-cyclohexylglycyl-glycyl-arginine-ρ-nitroanilide (SpecXa) was from American Diagnostica (Greenwich, CT). H-D-phenylalanyl-pipecolyl-arginine-ρ-nitroanilide, S-2765, and S-2222 were purchased from Chromogenix (West Chester, OH). Substrate solutions were prepared in water, and concentrations were verified using E_{342} = 8270 M^{-1} cm^{-1} (25). The affinity resin (AHV-5101-Seph) used to purify human FV from plasma and human thrombin were purchased from Hematologic Technologies (Essex Junction, VT). The calcium-dependent monoclonal human FX antibody (4G3 (26)) was obtained from Dr. Harold James (University of Texas, Tyler, TX). HEK 293 cells were obtained from ATCC (Manassas, VA). Tissue culture reagents were from Invitrogen. L-α-Phosphatidylserine (brain, sodium salt) and L-α-phosphatidylcholine (egg yolk) were purchased from Avanti Polarlipids (Alabaster, AL). Small unilamellar phospholipid vesicles composed of 75% (w/w) phosphatidylcholine and 25% (w/w) phosphatidylserine (PCPS) were prepared as described previously (27). The concentration of the phospholipid vesicles was determined by phosphorous assay (28).

Proteins—Human FX was isolated from fresh frozen plasma essentially as described (29). The FX activator ($RVV_{X\text{-}CP}$) was purified from crude venom of Russell's viper as described previously (30). Plasma-derived FV was isolated by immunoaffinity chromatography as described by Katzmann *et al.* (31) with minor modifications. Human FVa was prepared by proteolytic activation of FV by thrombin and purified as described (32). Plasma-derived human antithrombin III, recombinant tick anticoagulant peptide (rTAP) expressed in *Pichia Pastoris*, and recombinant prethrombin-2 expressed in Chinese hamster ovary cells were generous gifts from Dr. Sriram Krishnaswamy (The Joseph Stokes Jr. Research Institute, Philadelphia, PA). Molecular weights and extinction coefficients ($E^{0.1\%}_{280\ nm}$) of the various proteins used were taken as follows: $RVV_{X\text{-}CP}$, 93,000 and 1.18 (33); antithrombin III, 58,000 and 0.62 (34); prethrombin-2, 37,500 and 1.95 (35); thrombin, 37,500 and 1.94 (36); factor Va, 168,000 and 1.74 (37); factor X, 56,000 and 1.16 (38); factor Xa 45,300 and 1.16 (38).

Mutagenesis, Expression, and Purification of Recombinant FX—The recombinant FX mutant Tyr^{225} → Pro (FXa^{Y225P}) was generated with the QuikChange site-directed mutagenesis kit (Stratagene) using two complementary oligonucleotides containing the desired mutation, the sense strand being 5′-CGTAAGGGGAAGCCCGGGATCTACACC-3′. The entire FX cDNA was sequenced in order to confirm the presence of the desired mutation and to ensure that there were no polymerase-induced errors. Wild-type or mutant rFX in the mammalian expression plasmid pCMV4 were stably expressed in HEK 293 cells and purified as previously described (39, 40).

Activation of FX to FXa and Purification on Benzamidine-Sepharose—Plasma-derived FX (pdFX) and rFX were activated using $RVV_{X\text{-}CP}$ and subsequently purified using benzamidine-Sepharose or Sephacryl S-200 as described (39, 41). Following purification, plasma-derived and recombinant FXa molecules were precipitated, collected by centrifugation, dissolved in 50% glycerol, and stored at −20 °C.

Characterization of Plasma-derived and rFX/Xa—Protein purity was assessed using precast NuPAGE 4–12% Bis-Tris gels (Invitrogen) using the MES buffer system under reducing (50 mM dithiothreitol, final concentration) and nonreducing conditions followed by staining with Coomassie Brilliant Blue R-250. Gla analysis was carried out according to the modified method of Price (42) for alkaline hydrolysis. Separation of amino acids was accomplished using a DC-4A cation exchange column on a Waters LC-1 Plus high pressure liquid chromatograph (Milford, MA), and quantitation was done by postcolumn derivatization as described by Przysiecki (43). This analysis indicates that rwtFX and FX^{Y225P} have essentially the full complement of Gla residues (10.5–10.8 mol of Gla/mol of FX) compared with pdFX (10.7 mol of Gla/mol of FX; theoretical = 11 mol of Gla/mol of FX).

Determination of Kinetic Parameters for Peptidyl Substrate Hydrolysis—All kinetic measurements were performed in 20 mM Hepes, 0.15 M NaCl, 0.1% (w/v) polyethylene glycol 8000, 2 mM $CaCl_2$, pH 7.5 (assay buffer) unless otherwise indicated. The kinetics of peptidyl substrate hydrolysis (SpecXa, S-2765, and S-2222) was measured using increasing concentrations of substrate and initiated with either FXa or FXa assembled into prothrombinase.

Inhibition of FXa and Prothrombinase by PAB—The ability of PAB to bind to FXa or prothrombinase was assessed by two independent methods. In the first method, the inhibitory constant (K_i) of PAB for FXa or prothrombinase was assessed assuming classical competitive inhibition by initial velocity measurements of SpecXa hydrolysis by either enzyme using increasing concentrations of substrate at different fixed concentrations of PAB as previously described (44). In the second method, the binding of PAB to FXa or prothrombinase was directly assessed by fluorescence measurements essentially as described (45).

*Inhibition of FXa and Prothrombinase by rTAP and Determination of K_i**—Overall dissociation constants for rTAP binding to FXa and prothrombinase were inferred from measurements of residual enzyme amidolytic activity following incubation of the protease with increasing concentrations of the inhibitor essentially as described (46).

Inhibition of FXa and Prothrombinase by Antithrombin III—The rate of inactivation of FXa or prothrombinase by human antithrombin III was measured under pseudo-first order rate conditions. For the inhibition of FXa, human antithrombin III (0.16, 0.32, and 0.64 μM) was incubated with FXa (5 nM; FXa^{Y225P}, 10 nM) in assay buffer for up to 75 min (12 time points). At the end of the time course, 50 μl of SpecXa was added (100 μM final concentration) to monitor residual enzyme activity. For the inhibition of prothrombinase, human antithrombin III (1.6, 3.2, and 6.4 μM) was incubated with FXa (5 nM), FVa (50 nM), and PCPS (60 μM) in assay buffer for up to 30 min (12 points). Residual enzyme activity was monitored as described above. In both assays, each measurement was made in duplicate.

Functional Binding Studies: Measurement of Rates of Thrombin Generation—Apparent dissociation constants ($K_{d(app)}$) for FXa binding to FVa-PCPS were inferred from an assay measuring thrombin generation at various FVa concentrations as described previously (47). Assay mixtures contained PCPS (60 μM), FXa (5 nM), recombinant prethrombin-2 (2 μM), and FVa at various concentrations (0.7–54.0 nM) in assay buffer. The kinetic parameters of prothrombinase-catalyzed prethrombin-2 activation ($K_{m(app)}$ and V_{max}) were determined by measuring the initial rate of thrombin formation at increasing prethrombin-2 concentrations

as described (47). Assay mixtures contained PCPS vesicles (60 μM), FVa (30 nM), and various concentrations of recombinant prethrombin-2 (0–21 μM).

Functional Binding Studies: The Effect of FVa on Peptidyl Substrate Cleavage by FXa^{Y225P}—Reaction mixtures (200 μl) containing SpecXa (10–850 μM) and PCPS (60 μM) with different fixed concentrations of FVa (0.5, 1.0, 2.0, 3.0, 5.0, 10, and 20 nM) were prepared in the wells of a 96-well plate and allowed to incubate for 5 min at room temperature. Because the substrate stock solution was prepared in water, an appropriate volume of 10× assay buffer solution adjusted to pH 7.75 was added to each mixture to ensure that the final pH and concentration of buffer solutes were invariant. The reaction was initiated with FXa^{Y225P} (3 nM final concentration).

Carbamylation of Ile^{16} by Reaction with NaNCO—Mixtures containing FXa^{Y225P} or pdFXa (1–2 μM) in assay buffer were incubated in the presence or absence of different fixed concentrations of PAB (50–2200 μM; 10 concentrations) and were reacted with either 0.2 or 0.6 M NaNCO. The final pH of the reaction mixture upon the addition of NaNCO was pH 7.45. At selected time intervals (5–300 min), 5 μl of the reaction mixture was placed in 95 μl of assay buffer, and the residual enzymatic activity was determined from initial steady state rates of SpecXa hydrolysis, or aliquots were mixed with 1.5 M hydroxylamine, pH 8.0, and then frozen at −80 °C for N-terminal sequence analysis. Amino-terminal sequence analysis was performed in the laboratory of Dr. Jan Pohl (Emory University Microchemical Facility). Quenched protein samples at various time points (40 pmol) were mixed with rTAP (20 pmol; internal protein control) and spotted onto polyvinylidene difluoride membranes, and N-terminal sequence analysis was performed using an automated PE-Biosystems 491A pulsed liquid sequencer on-line with a PE-Biosystems 140S PTH analyzer. The peak area (in pmol) of PTH-Ile (first cycle of the heavy chain of FXa) and PHT-Tyr (first cycle of rTAP) were determined simultaneously. Control experiments included incubating the mutant protein as described above but in the presence of 0.2 M NaCl.

Data Analysis—Data were analyzed according to the indicated equations by nonlinear least squares regression analysis using the Marquardt algorithm (48). The qualities of the fits were assessed by the criteria described (49). Fitted parameters are reported ± 95% confidence limits.

Determination of Steady State Kinetic Constants—Initial velocity measurements of peptidyl substrate or macromolecular substrate (prethrombin-2) hydrolysis by FXa or prothrombinase were analyzed by fitting the data to the Henri-Michaelis-Menten equation (50) to yield fitted values for K_m and V_{max}.

Inhibition Studies—Initial velocity measurements of SpecXa hydrolysis by FXa or prothrombinase using increasing concentrations of substrate at different fixed concentrations of PAB were analyzed according to the rate expression for linear competitive inhibition (50) to yield the fitted values for K_m, V_{max}, and K_i. Initial velocity data obtained following incubation of increasing concentrations of rTAP with two fixed concentrations of FXa or prothrombinase were analyzed as described (45). Data derived from direct fluorescence binding measurements between PAB and FXa and PAB and prothrombinase were analyzed as described previously (45) taking into account the inner filter effect (51). The rate of inhibition of FXa or prothrombinase by antithrombin III was measured under pseudo-first order rate conditions, and the second order rate constant was calculated by dividing the pseudo-first order rate constant by the concentration of antithrombin III.

Equilibrium Constant for Prothrombinase Assembly—Dissociation constants and stoichiometries for the interaction between FXa and PCPS-bound FVa were obtained from the dependence of the initial rate on the concentrations of factor Va (52).

Global Analysis of Initial Velocity Data: Effect of FVa on Peptidyl Substrate Cleavage by FXa^{Y225P}—The equilibrium dissociation constants for the binding of FVa to membrane-bound FXa in the absence (K_{d1}) and presence of peptidyl substrate (K_{d2}) as well as the substrate dissociation constant for FXa (K_{s1}) and membrane-bound FXa saturated with FVa (K_{s2}) were calculated from initial velocity measurements of SpecXa hydrolysis at different fixed concentrations of FVa according to the system of ordinary differential equations describing Scheme I and using the rapid equilibrium assumption. The entire data set was globally fit using the program Dynafit (53) to extract K_{s1}, k_{cat1}, K_{d1}, K_{s2}, K_{d2}, and k_{cat2}.

Carbamylation of FXa in the Presence of PAB: Global Analysis of First Order Inactivation Rate Constants—The first order rate inactivation constant for FXa by NaNCO in the absence of PAB (k_0) and in the presence of saturating concentrations of PAB (k_1) as well as the equilibrium dissociation constant (K_d) for PAB binding to FXa were calculated by globally fitting activity data as a function of time to the ordinary differential equations describing the reaction mechanism shown in Scheme II using the program Dynafit (53) to extract K_d, k_0, and k_1.

RESULTS

Expression and Purification of Recombinant Proteins—rwtFX and FX^{Y225P} were expressed in HEK 293 cells and purified to homogeneity. Following activation with RVV$_{X\text{-}CP}$, each protein was applied to benzamidine-Sepharose. Whereas native FXa bound and was eluted from the column with 4 mM benzamidine, FXa^{Y225P} did not bind to the resin (data not shown). These findings suggest that FXa^{Y225P} has a reduced ability to bind benzamidine at the S1 specificity pocket. The mutant protein was subsequently purified by gel filtration. SDS-PAGE analysis of the purified zymogens (*lanes 1–3*) and purified proteases (*lanes 4* and *5*) before and after disulfide bond reduction are shown in Fig. 1.

Assessment of Binding at the Active Site—As detailed previously, the ability of GDFXa^{Y225P} to cleave small peptidyl substrates is impaired, as is that of wild-type FXa in the absence of Na^+ (9, 18). Consistent with these observations, an increase in the K_m for peptidyl substrates and a decrease in the k_{cat} compared with wild-type FXa was observed for full-length FXa^{Y225P} (Table I). These data indicate that the mutant protein has altered activity and suggest that the substrate binding cleft (S1–S3 site) is changed in some fashion. Similar results were obtained with rFXa^{Y225P} bound to PCPS vesicles (data not shown; also see Fig. 3). In contrast to these results, the assembly of FXa^{Y225P} into prothrombinase restored the K_m for peptidyl substrates to that seen with wild-type proteins, whereas the k_{cat} values were not significantly altered (Table I). At present, it is unclear why the k_{cat} was reduced by a factor of 1.5–5 for both FXa^{Y225P} and this mutant assembled in prothrombinase with the various peptidyl substrates. The data are consistent with the conclusion that prothrombinase complex assembly appears to correct defective binding of peptidyl substrates to the mutant protein.

Since changes in the K_m for peptidyl substrates could arise from a variety of effects, the binding of a well defined S1 probe, PAB, to FXa was also investigated. Whereas the wild-type proteins bound PAB with essentially identical affinities, FXa^{Y225P} had a ~10-fold reduced affinity for PAB, indicating the S1 specificity pocket of the mutant is altered (Table II). These data are consistent with the reduced affinity of PAB observed previously for wild-type FXa in the absence of Na^+ (9). In contrast, assembly of the mutant with saturating concentrations of FVa and membranes restored PAB binding to that seen with wild-type FXa assembled in prothrombinase (Table II). Similar results were also obtained with both rTAP and antithrombin III. Together, these results indicate that prothrombinase complex assembly, in the context of an altered Na^+-binding site, appears to modify the affinity of active site-directed probes.

Cleavage of the Macromolecular Substrate Prethrombin-2—Assuming that the substrate exosite is not changed in any fashion, the above data would suggest that rates of cleavage of the macromolecular substrate, prethrombin-2, by FXa^{Y225P} assembled in prothrombinase would be similar to wild-type prothrombinase. Initial velocity measurements with saturating concentrations of FVa and membranes indicate that this is indeed the case (Fig. 2). Fitting the data to the Michaelis-Menten equation indicates that the mutant assembled in prothrombinase has similar kinetic parameters for prethrombin-2 (K_m = 4.35 ± 0.26 μM; k_{cat} = 0.561 ± 0.1 s^{-1}; k_{cat}/K_m = 0.129 μM^{-1} s^{-1}) compared with wild-type prothrombinase (pdFXa, K_m = 8.35 ± 0.69 μM, k_{cat} = 1.56 ± 0.05 s^{-1}, k_{cat}/K_m = 0.190

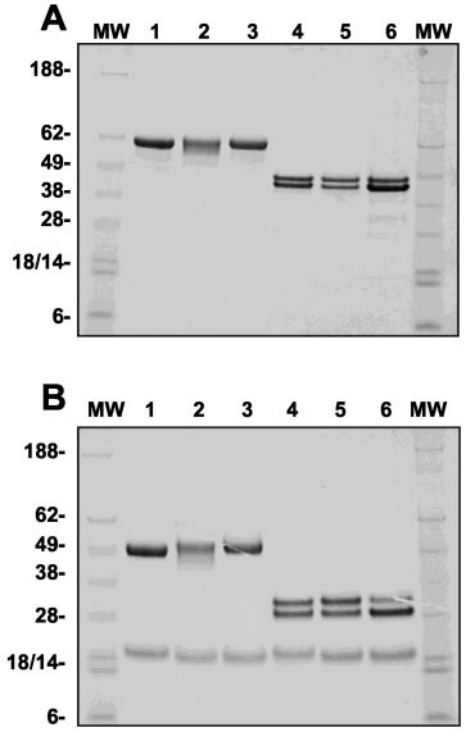

FIG. 1. **SDS-PAGE analysis of purified factor X and factor Xa.** Purified proteins (3 μg/lane) were subjected to SDS-PAGE without (*A*) or with disulfide bond reduction (*B*) (50 mM dithiothreitol) and visualized by staining with Coomassie Brilliant Blue R-250. *Lane 1*, human pdFX; *lane 2*, rwtFX; *lane 3*, FX^{Y225P}; *lane 4*, human pdFXa; *lane 5*, rwtFXa; *lane 6*, FXa^{Y225P}. The apparent molecular weights of the standards are indicated on the *left*.

TABLE I
Kinetic constants for the cleavage of peptidyl substrates by factor Xa and prothrombinase

For experiments in which free factor Xa was used, 2.0 nM wild-type or 6.0 nM mutant factor Xa was incubated with increasing concentrations of substrate, and for experiments in which prothrombinase was employed 5.0 nM wild-type or mutant factor Xa was incubated with 30 nM factor Va, 50 μM PCPS, and increasing concentrations of substrate (10–500 μM) as described under "Experimental Procedures." The errors in the fitted constants represent 95% confidence limits. Data are representative of two or three similar experiments.

Substrate	Enzyme species[a]	$K_m \pm$ S.D.	$k_{cat} \pm$ S.D.
		μM	s^{-1}
Free factor Xa			
SpecXa	PDFXa	97 ± 4.4	210 ± 3.3
	rwtFXa	85 ± 6.5	198 ± 18
	$rFXa^{Y225P}$	814 ± 154	54 ± 7.1
S-2222	PDFXa	170 ± 6.8	100 ± 1.6
	rwtFXa	148 ± 9.9	98 ± 2.4
	$rFXa^{Y225P}$	1607 ± 37	38 ± 6.9
S-2765	PDFXa	50 ± 6.2	202 ± 6.8
	rwtFXa	37 ± 7.4	191 ± 9.1
	$rFXa^{Y225P}$	1102 ± 231	139 ± 22
Prothrombinase			
SpecXa	PDFXa	192 ± 6.7	220 ± 3.3
	rwtFXa	181 ± 13	198 ± 6.1
	$rFXa^{Y225P}$	174 ± 6.4	43 ± 0.7
S-2222	PDFXa	301 ± 27	88 ± 4.1
	rwtFXa	353 ± 44	91 ± 6.3
	$rFXa^{Y225P}$	323 ± 28	20 ± 0.9
S-2765	PDFXa	145 ± 9.9	258 ± 7.1
	rwtFXa	136 ± 8.6	242 ± 6.0
	$rFXa^{Y225P}$	139 ± 18	58 ± 2.9

$\mu M^{-1}\ s^{-1}$; rwtFXa, $K_m = 9.07 \pm 0.91\ \mu M$, $k_{cat} = 1.54 \pm 0.06\ s^{-1}$, $k_{cat}/K_m = 0.170\ \mu M^{-1}\ s^{-1}$). Consistent with results obtained with peptidyl substrates, the k_{cat} for macromolecular substrate cleavage by the mutant assembled in prothrombinase was moderately reduced. These data are in contrast to those using GDFXa in the absence of Na^+ or $GDFXa^{Y225P}$, where the rate of prethrombin-1 activation was dramatically impaired (18).

TABLE II
Inhibition kinetics of synthetic peptidyl substrate cleavage by factor Xa or prothrombinase

Inhibitor[a]	PAB[b] $K_i \pm$ S.D.	rTAP $K_i \pm$ S.D.	Antithrombin III $k_2 \pm$ S.D. $\times 10^3$
	μM	nM	$M^{-1}\ s^{-1}$
Free FXa			
PDFXa	55 ± 3.3	0.13 ± 0.04	2.76 ± 0.13
rwtFXa	57 ± 3.7	0.14 ± 0.04	2.73 ± 0.15
$rFXa^{Y225P}$	481 ± 21	21.3 ± 2.4	0.22 ± 0.01
Prothrombinase			
PDFXa	63 ± 3.3	0.036 ± 0.003	0.38 ± 0.29
rwtFXa	59 ± 2.4	0.031 ± 0.003	0.36 ± 0.15
$rFXa^{Y225P}$	87 ± 6.9	0.029 ± 0.002	0.29 ± 0.20

[a] Inhibition kinetics of factor Xa alone or prothrombinase were determined from initial velocity studies conducted with the peptidyl substrate, SpecFXa or IEGR-AMC. Details of experimental design and concentrations of reactants can be found under "Experimental Procedures."

[b] The binding of PAB to the various FXa or prothrombinase species was determined kinetically (K_i) and by fluorescence measurements (K_d). Essentially identical results were found between the two methods. The errors in the fitted constants represent 95% confidence limits. Data are representative of two or three similar experiments.

Assessment of Thermodynamic Linkage—The data indicate that the binding of FVa to membrane-bound FXa^{Y225P} appears to enhance binding of molecules that target the S1 site (Tables I and II). This implies that a thermodynamic linkage exists between the FVa, S1, and Na^+-binding sites. Experiments were designed such that all relevant equilibrium binding constants depicted in Scheme I could be simultaneously evaluated.

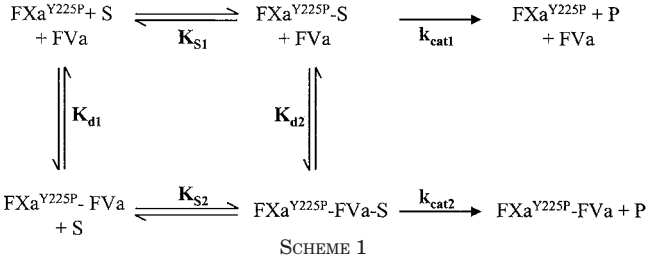

SCHEME 1

In this model, FXa^{Y225P} and FVa are membrane-bound, and S represents SpecXa. A signal to monitor the various binding interactions was provided by the difference in chromogenic activity between FXa^{Y225P} and the mutant saturated with FVa and membranes (Table I). Initial velocity measurements of SpecXa cleavage by membrane-bound FXa^{Y225P} at different fixed concentrations of FVa (Fig. 3) were made, followed by global analysis of all relevant equations describing the binding interactions depicted in Scheme I. The data indicate that membrane-bound FXa^{Y225P} binds with a decreased affinity to FVa ($K_{d1} = 26.0 \pm 5.4$ nM) and peptidyl substrates ($K_{s1} = 695 \pm 49\ \mu M$) compared with wild-type FXa; however, occupation of the S1 site restored FVa binding ($K_{d2} = 2.1 \pm 0.26$ nM), and saturating membrane-bound FXa^{Y225P} with FVa restored peptidyl substrate binding ($K_{s2} \approx 56\ \mu M$). These data imply that there is allosteric linkage between the Na^+, FVa, and S1 sites (*i.e.* the binding of FVa to FXa^{Y225P} enhances the binding of molecules that target the S1 site and *vice versa*). The rates of catalysis of FXa^{Y225P} in the absence of FVa ($k_{cat1} = 43 \pm 1.6\ s^{-1}$) or in the presence of saturating concentrations of FVa ($k_{cat2} = 41 \pm 0.7\ s^{-1}$) are essentially the same, indicating that

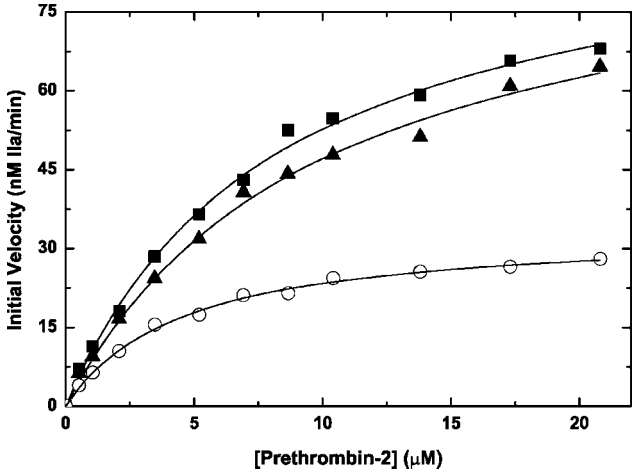

FIG. 2. **Determination of kinetic constants for cleavage of prethrombin-2 by prothrombinase.** The initial velocity of thrombin generation was determined at increasing concentrations of prethrombin-2 with 5.0 nM prothrombinase (5.0 nM FXa, 30 nM FVa, and 60 μM PCPS) in assay buffer (pdFXa (■), rwtFXa (▲), or FXa^{Y225P} (○)). The data points represent the average of duplicate measurements (S.D. < 10%), and the data are representative of two similar experiments. The *lines* were drawn following analysis of all data sets to the Henri-Michaelis-Menten equation using the fitted parameters: pdFXa, K_m = 8.35 ± 0.69 μM, k_{cat} = 1.56 ± 0.05 s^{-1}; rwtFXa, K_m = 9.07 ± 0.91 μM, k_{cat} = 1.54 ± 0.06 s^{-1}; and FXa^{Y225P}, K_m = 4.35 ± 0.26 μM, k_{cat} = 0.561 ± 0.01 s^{-1}.

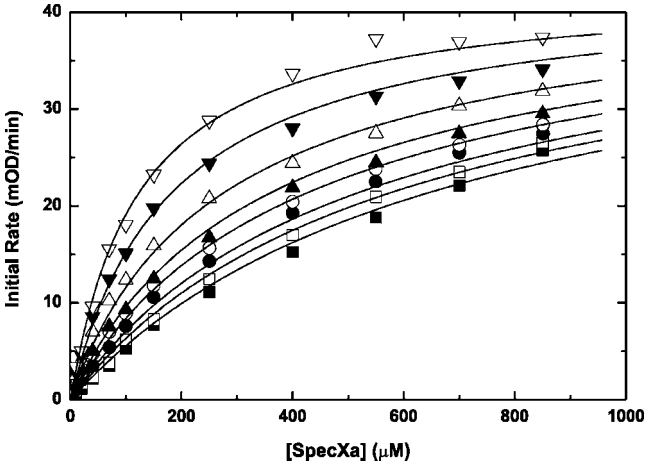

FIG. 3. **Effect of factor Va on peptidyl substrate cleavage by membrane-bound factor Xa^{Y225P}.** The initial velocity of peptidyl substrate hydrolysis catalyzed by membrane-bound FXa^{Y225P} (3 nM; 60 μM PCPS) was determined using increasing concentrations of SpecXa in the presence of different fixed concentrations of FVa (0 nM (■), 0.5 nM (□), 1.0 nM (●), 2.0 nM, (○), 3.0 nM, (▲), 5.0 nM, (△), 10.0 nM (▼), and 20.0 nM (▽)) in assay buffer. The data are representative of two similar experiments. The lines are drawn following global analysis of initial velocity data as described under "Data Analysis" using the fitted parameters (see Scheme I): K_{d1} = 26.0 ± 5.4 nM; K_{s1} = 695 ± 49 μM; K_{d2} = 2.1 ± 0.26 nM; $K_{s2} \approx$ 56 μM; k_{cat1} = 43 ± 1.6 s^{-1}; and k_{cat2} = 41 ± 0.7 s^{-1}.

the binding of FVa to FXa^{Y225P} does not influence the rate constant for peptidyl substrate hydrolysis.

Additional experiments were also performed aimed at assessing the FXa^{Y225P}-FVa interaction using the macromolecular substrate, prethrombin-2. Measurements of the conversion of a single fixed concentration of prethrombin-2 to thrombin were conducted using increasing concentrations of FVa at a single, fixed concentration of FXa and PCPS (Fig. 4). Because of the experimental conditions chosen and the very high K_m of membrane-bound FXa for prethrombin-2 (47), the equilibrium dissociation constant measured in the following experiment is

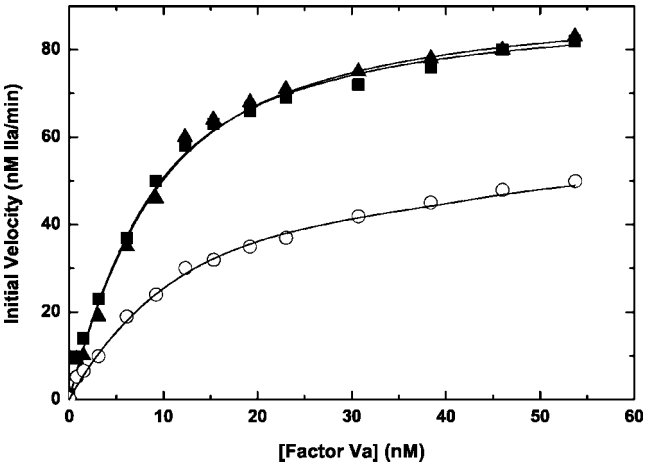

FIG. 4. **Dependence on the rate of cleavage of prethrombin-2 on prothrombinase assembly.** Reaction mixtures containing 2.0 μM prethrombin-2, 60 μM PCPS, and the indicated concentrations of FVa in assay buffer were initiated with 5.0 nM FXa (pdFXa (■), rwtFXa (▲), or FXa^{Y225P} (○)). The data points represent the average of duplicate measurements (S.D. < 10%), and the data are representative of two similar experiments. Initial velocities determined as a function of FVa were analyzed using the equations and assumptions described under "Data Analysis" using the fitted parameters: pdFXa, K_{d1} = 6.2 ± 0.4 nM; rwtFXa, K_{d1} = 6.3 ± 0.5 nM; and FXa^{Y225P}, K_{d1} = 17.3 ± 1.1 nM.

expected to be analogous to K_{d1} depicted in Scheme I. The inferred equilibrium dissociation constant for membrane-bound FVa binding to FXa^{Y225P} (K_{d1} = 17.3 ± 1.1 nM) was ~3-fold greater than that observed with the wild-type proteins (pdFXa, K_{d1} = 6.2 ± 0.4 nM; rwtFXa, K_{d1} = 6.3 ± 0.5 nM, assuming a stoichiometry of 1). These results are in reasonable agreement with K_{d1} obtained using peptidyl substrates.

Modification of the N-terminal Ile^{16}—A possible explanation for the apparent altered S1- and FVa-binding sites on FXa^{Y225P} is that mutation at the Na^+-binding site destabilizes the salt bridge between Ile^{16} and Asp^{194}, thereby favoring a zymogen-like conformation. In order to test this idea, FXa^{Y225P} was reacted with NaNCO, which preferentially modifies the N terminus on proteins and to a lesser extent α-amino groups on lysines (54, 55). The results indicate that the rate of inactivation by NaNCO of FXa^{Y225P} was 6-fold faster compared with wild-type FXa (second-order rate constants, 45.0 mM^{-1} min^{-1} *versus* 7.50 mM^{-1} min^{-1}; Fig. 5, *closed symbols*). Whereas cyanate has been used to investigate the susceptibility of the N terminus of FVIIa (Ile^{16}) to be chemically modified by activity and sequencing methods (56, 57), it is possible that the reduction in activity of FXa^{Y225P} may be unrelated to modification of the N terminus. To address this issue, FXa^{Y225P} was incubated with cyanate, and the rate of disappearance of PTH-Ile^{16} derived from the N terminus of the heavy chain was monitored over time. To control for internal inconsistencies in the sequencing set-up and reaction, an internal protein standard (rTAP) was included, and the values of PTH-Ile^{16} (N terminus of heavy chain of FXa) to PTH-Tyr (N terminus of rTAP) was expressed as a ratio. Consistent with activity measurements, the rate of carbamylation of FXa^{Y225P} was 6.8-fold faster compared with wild-type FXa using the sequencing method (second-order rate constants, 41.0 mM^{-1} min^{-1} *versus* 6.01 mM^{-1} min^{-1}; Fig. 5, *open symbols*), indicating that the loss in activity correlates very well with modification of the N-terminal Ile^{16}.

It is well documented for trypsin that formation of the Ile^{16}–Asp^{194} internal salt-bridge is allosterically linked to the S1 specificity site (58). Since FXa^{Y225P} appears to have a partially destabilized N-terminal insertion, occupation of the S1 site of FXa^{Y225P} should stabilize the Ile^{16}–Asp^{194} salt bridge. FXa^{Y225P} in the presence of several fixed concentrations of PAB

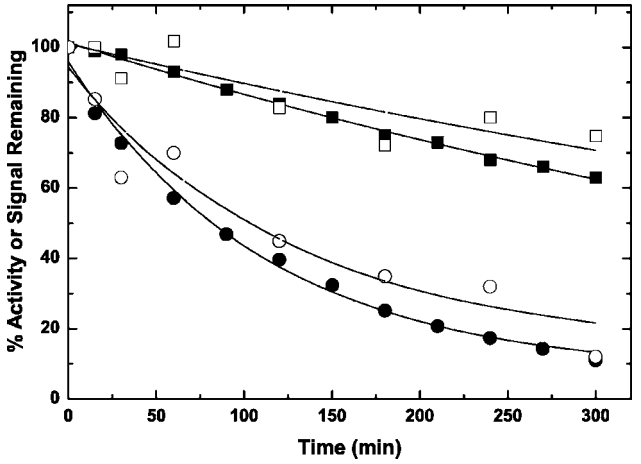

FIG. 5. **Carbamylation of FXa and FXa^{Y225P} by NaNCO.** Reaction mixtures containing 2.0 μM of plasma-derived FXa (*squares*) or FXa^{Y225P} (*circles*) in assay buffer adjusted to pH 7.0 were reacted with 0.2 M NaNCO. At selected time intervals (0, 15, 30, 60, 90, 120, 150, 180, 210, 240, 270, and 300 min), an aliquot of the reaction mixture was either mixed with assay buffer and the remaining enzymatic activity was determined from initial steady state rates of SpecXa hydrolysis (*closed symbols*) or aliquots were mixed with 1.5 M hydroxylamine, pH 8.0, and then frozen at −80 °C for N-terminal sequence analysis as described under "Experimental Procedures" (*open symbols*). The percentage of residual activity or signal remaining was plotted as a function of time upon incubation with NaNCO. Data derived from activity measurements (*closed symbols*) are representative of four similar experiments, whereas data derived from the sequence analysis (*open symbols*) represent a single experiment. The *lines* are drawn according to rate expressions described under "Data Analysis" using the fitted parameters: pdFXa, 7.50 ± 1.49 mM^{-1} min^{-1}; FXa^{Y225P}, 45.0 ± 1.58 mM^{-1} min^{-1} (*closed symbols*); pdFXa, 6.01 ± 0.88 mM^{-1} min^{-1}; FXa^{Y225P}, 41.0 ± 7.3 mM^{-1} min^{-1} (*open symbols*).

was reacted with NaNCO over an extended time course (Fig. 6*A*). Global analysis of all data sets to equations describing all relevant interactions depicted in Scheme II (where P represents PAB) permitted the determination of the equilibrium dissociation constant (K_d) for PAB-FXa^{Y225P} and the second order rate constants for the modification of FXa^{Y225P} by NaNCO in the absence (k_0) and presence (k_1) of saturating PAB (*FXa^{Y225P} indicates that it has been covalently modified at the N terminus with NaNCO). Inspection of the observed rate constants (k_{obs}, derived from Fig. 6*A*) as a function of the PAB concentration (Fig. 6*B*) indicates that the interaction of FXa^{Y225P} with PAB is relatively weak (K_d = 726 ± 53 μM), results that are in agreement with direct binding fluorescence and kinetic measurements (Table II). Additionally, saturation of FXa^{Y225P} by PAB afforded complete protection of the enzyme from carbamylation, as evident by an extremely small second order rate constant ($k_1 = <1 \times 10^{-5}$ mM^{-1} min^{-1}) compared with FXa^{Y225P} in the absence of PAB (k_0 = 39.0 ± 1.28 mM^{-1} min^{-1}). These data indicate that occupation of the S1 site of the variant results in stabilization of the N-terminal insertion and resistance of the enzyme to carbamylation. These results also support the idea that the reduction in activity observed with FXa^{Y225P} in the presence of cyanate is related to modification of the N terminus, since the loss in activity could be reversed upon occupation of the S1 site (Fig. 6).

$$\begin{array}{ccc} \text{FXa}^{Y225P} + \text{P} + \text{NaNCO} & \underset{}{\overset{K_d}{\rightleftharpoons}} & \text{FXa}^{Y225P}\text{-P} + \text{NaNCO} \\ \Big\downarrow k_0 & & \Big\downarrow k_1 \\ *\text{FXa}^{Y225P}\text{- NaNCO} + \text{P} & & *\text{FXa}^{Y225P}\text{-P-NaNCO} \end{array}$$

SCHEME 2

DISCUSSION

The zymogen to protease transition in the trypsin-like serine protease family of proteins is initiated following proteolytic liberation of a highly conserved N terminus and removal of an activation peptide. As shown for the trypsinogen/trypsin system, a new free α-amino group (Ile^{16}) forms a salt bridge with the Asp^{194} carboxylate group following activation that either results in or is associated with a conformational change in the so-called "activation domain" (residues comprising positions 16–19, 142–152, 184–194, and 216–223) (59, 60). Since N-terminal insertion is energetically linked to the maturation of the activation domain, alteration of any of these structural elements including the S1 specificity pocket should positively or negatively influence the others.

The results of the current study indicate that alteration of the FXa Na^+-binding site by changing residue 225 from a Tyr to a Pro results in the transformation of this serine protease from a protease-like state to a zymogen-like state, providing a reasonable explanation for the observations of reduced activity (this study and Ref. 18). This shift in favor to the zymogen-like state results from destabilization of the N terminus (Ile^{16}) of FXa^{Y225P} and adversely affects FVa binding and binding of substrates to the S1 specificity pocket. Consistent with thermodynamic principles, protection of the N-terminal Ile^{16} from modification was achieved by saturation of the S1 specificity site with PAB, thereby favoring the active or protease-like conformation (Fig. 6). Additionally, saturation of membrane-bound FXa^{Y225P} with FVa also assisted the variant to adopt a more protease-like state, suggesting that the FVa and Na^+-binding sites are allosterically linked (Figs. 2–4). These findings are consistent with the well documented zymogen to protease transition in trypsinogen/trypsin (61) (*i.e.* the zymogen state and the protease state exist in an equilibrium that can be shifted depending on environmental conditions (*e.g.* various ligands)).

At present, it is not clear whether the activity of free FXa is modulated by Na^+ *in vivo*, since there are conflicting reports on the dissociation constant of Na^+ for calcium-bound FXa (9, 18, 21). Additionally, it is unlikely that the levels of Na^+ would change significantly enough to influence the activity of FXa, since the Na^+ concentration is tightly regulated. However, if Na^+-bound and Na^+-free forms of FXa are equally populated *in vivo*, then these forms of the enzyme would be sensitive to changes in the availability of allosteric effector molecules that are linked to the Na^+-binding site. These changes could influence a variety of reactions in which FXa participates (*e.g.* activation of FV, FVII, cellular receptors, and interactions with TFPI and ATIII). With respect to prothrombin activation, the current data indicate that once membrane-bound FXa^{Y225P} is saturated with FVa, the rate of macromolecular substrate cleavage is similar to native prothrombinase, calling into question the physiological significance of Na^+ in influencing this reaction. However, as the catalytic activity of prothrombinase appears to be insensitive to changes at the FXa Na^+-binding site (Fig. 2), the binding of membrane-bound rFXa^{Y225P} to FVa is adversely affected (Figs. 3 and 4). Thus, whereas the overall rate of thrombin generation by prothrombinase may be influenced by changes at the FXa Na^+-binding site, the degree of this change would depend upon the amount of FVa available and possibly other factors that could influence the equilibrium between the two forms of the enzyme.

The FXa Na^+ and S1 specificity sites are part of the so-called activation domain and would presumably be disordered in the

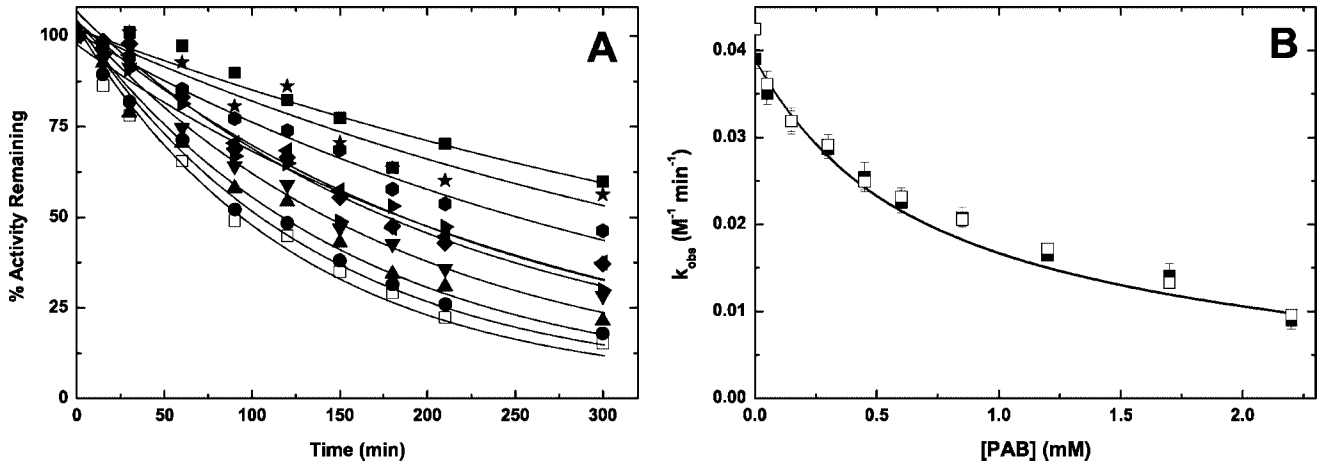

FIG. 6. **The effect of active site occupation by PAB on the rate of carbamylation of FXa^{Y225P} by NaNCO.** *A*, reaction mixtures containing FXa^{Y225P} (800 nM) in assay buffer adjusted to pH 7.0 were incubated with different fixed concentrations of PAB (0 (□), 50, 150, 300, 450, 600, 850, 1200, 1700, and 2200 (■) μM) and reacted with 0.2 M NaNCO. At selected time intervals (0, 15, 30, 60, 90, 120, 150, 180, 210, and 300 min), an aliquot of the reaction mixture was mixed with assay buffer, and the remaining enzymatic activity was determined from initial steady state rates of SpecXa hydrolysis and plotted as a function of time of incubation with NaNCO. *B*, individual observed rate constants (k_{obs}, error bars represent the S.D. of the calculated rate constant) at any given concentration of PAB derived from *A* (note that k_{obs} is given as per M inhibitor (NaNCO) concentration; *closed squares*, experiment with 0.2 M NaNCO; *open squares*, experiment with 0.6 M NaNCO) were plotted as a function of the PAB concentration. The data are representative of three similar experiments. The *lines* in both *panels* are drawn according to rate expressions described under "Data Analysis" using the fitted parameters (see Scheme II): $k_0 = 39.0 \pm 1.28$ mM^{-1} min^{-1}; $k_1 = <1 \times 10^{-5}$ mM^{-1} min^{-1}; and $K_d = 726 \pm 53$ μM.

zymogen and become ordered upon N-terminal insertion. A recently described model of the zymogen FX suggests that this may be the case (62). Comparison of the zymogen model with the active enzyme reveals that residues making up the calcium (Asp^{70}–Glu^{80}), sodium (Ala^{183}–Asp^{194}; Gly^{219}–Gly^{226}) and autolysis loops (Thr^{144}–Arg^{150}) undergo major changes in their backbone positions upon the zymogen to protease transition. These results suggest that these regions in FX are at least influenced by this transition. Since it is already well documented, at least for trypsinogen/trypsin, that the S1 specificity site and formation of Ile^{16}–Asp^{194} are allosterically linked, it is reasonable to hypothesize that other elements of the activation domain are also linked to the zymogen to protease transition. By definition, this means that alterations at the Na^+ binding site, for example, will influence the formation of the Ile^{16}–Asp^{194} salt bridge, consistent with observations of the current study (Figs. 5 and 6).

The idea that changes at the Na^+-binding site can influence ion pair formation is in agreement with recent findings indicating that an increase in the pH results in a decrease in the Na^+ affinity for several serine proteases, including FXa (63). It was hypothesized that deprotonation of an ion pair ($pK_a \approx 9.2$; assumed, but not proven to be Ile^{16}–Asp^{194}) by changes in pH will result in a break of the salt bridge and yield an internal disruption of the Na^+-binding site. Whereas it is clear that large changes in the pH capable of disrupting ion pair formation cannot be a mechanism by which the FXa Na^+-binding site is modulated *in vivo*, the study nevertheless provides evidence that formation of the Ile^{16}–Asp^{194} salt bridge appears crucial in the stabilization of the architecture of the Na^+-binding site.

Thus, a key aspect of the zymogen to protease transition for serine proteases that are sensitive to Na^+ may be the formation of a functional Na^+-binding site. This model would predict that the Na^+ site of the zymogen binds the cation with a very weak affinity; high affinity binding would follow activation of the zymogen and ordering of the Na^+ site. Support for this idea comes from the current study as well as other studies. For example, inspection of the crystal structure of the homologous zymogen prethrombin-2 in complex with hirugen reveals that, in contrast to thrombin, there are several key movements of loop segments and critical groups in the vicinity of the Na^+ site that would prevent Na^+ binding to the zymogen, consistent with its apparent absence in the prethrombin-2 structure (11, 64). The same also appears to be true with the recently described FVII zymogen structure, which demonstrates that loop regions making up the Na^+-binding site (184–193 and 215–224) are shifted up to 12 Å compared with the tissue factor/FVIIa structure (65). Additionally, using a direct fluorescence binding assay, De Cristofaro *et al.* (16) were not able to detect Na^+ binding to protein C, suggesting that the Na^+ site in this zymogen is exposed only after its activation.

In addition to disruption of the N-terminal insertion and S1 specificity pocket, mutation at the Na^+ site also results in decreased cofactor binding, suggesting that the FVa binding site is allosterically linked to elements in the activation domain. The data indicate that occupation of the S1 specificity site of membrane-bound FXa^{Y225P} enhances binding at the FVa binding site and *vice versa*, explaining well why these two enzymes (FXa^{Y225P} and mutant prothrombinase) have different reactivities toward active site-directed probes (Tables I and II; see Scheme I). In contrast to these observations, the binding of membrane-bound FVa to wild-type FXa is accompanied by a minor change in active site function (66, 67). A possible explanation for this is that linkage between the FVa and S1 binding sites is obscured in wild-type FXa, because the protease-like conformation is highly favored. In contrast, FXa^{Y225P}, with an altered Na^+-binding site, exists in a zymogen-like conformation, thereby making linkage between the FVa and S1 sites more discernible. This explanation would appear consistent with the observation that the zymogen FX does not detectably bind FVa or S1-directed probes.

A possible alternative explanation to allosteric linkage is that steric factors are influencing the affinity of FVa for membrane-bound FXa^{Y225P}. For example, disruption of the Ile^{16}–Asp^{194} salt bridge in FXa^{Y225P} could result in movement of the N-terminal segment such that it sterically hinders the binding of FVa to membrane-bound FXa^{Y225P}. Implicit in this argument is that the enzyme exists in two states, one in which the N terminus blocks the FVa binding site and one in which the site is accessible. Any molecule that facilitates the formation of the Ile^{16}–Asp^{194} salt bridge (*e.g.* binding of S1 probes) would shift the equilibrium between the two states, removing this

steric factor and restoring FVa binding. At present, this scenario cannot be formally ruled out, and future studies are needed to distinguish between the two possibilities.

Examination of the FXa crystal structure in the vicinity of the putative FVa binding helix (68), Na^+ site, and S1 specificity site may provide, however, some insight into how these elements could be allosterically linked at the structural level. As previously noted (9, 11), the Na^+ site in FXa is linked to the S1 specificity site (specifically Asp^{189}) via two water molecules. The FVa binding helix (residues 162–169) is connected to the Na^+-binding site through van der Waals' contacts between Tyr^{225} and Val^{163} and between the OH group of Tyr^{225} and (via two water molecules) Ser^{167}. When the FXa Tyr^{225} to Pro mutation was modeled (9) the results indicate that its carbonyl oxygen atom would point away from the Na^+-binding site and that its side chain would be unable to make contacts with the FVa binding helix. The data of the current study are consistent with this model. Future experiments aimed at preventing internal salt bridge formation should provide further evidence that the FVa, S1, and Na^+-binding sites consist of a structural network allosterically linked to the zymogen to protease transition.

Acknowledgments—I am grateful to Dr. Katherine A. High and to Dr. Sriram Krishnaswamy of The Joseph Stokes Research Institute, Children's Hospital of Philadelphia and The University of Pennsylvania for reading the manuscript and making critical comments and useful suggestions. I am also grateful to Dr. Jan Pohl (Emory University Microchemical Facility) for N-terminal sequence analysis.

REFERENCES

1. Watzke, H. H., and High, K. A. (1995) in *Molecular Basis of Thrombosis and Hemostasis* (High, K. A., and Robert, H. R., eds) pp. 239–255, Marcel Dekker, Inc., New York
2. Mann, K. G., Nesheim, M. E., Church, W. R., Haley, P., and Krishnaswamy, S. (1990) *Blood* **76,** 1–16
3. Furie, B., and Furie, B. C. (1976) *J. Biol. Chem.* **251,** 6807–6814
4. Orthner, C. L., and Kosow, D. P. (1978) *Arch. Bioch. Biophys.* **185,** 400–406
5. Sugo, T., Bjork, I., Holmgren, A., and Stenflo, J. (1984) *J. Biol. Chem.* **259,** 5705–5710
6. Persson, E., Hogg, P. J., and Stenflo, J. (1993) *J. Biol. Chem.* **268,** 22531–22539
7. Rezaie, A. R., and Esmon, C. T. (1994) *J. Biol. Chem.* **269,** 21495–21499
8. Sabharwal, A. K., Padmanabhan, K., Tulinsky, A., Matoth, Y., Gorka, J., and Bajaj, S. P. (1997) *J. Biol. Chem.* **272,** 22037–22045
9. Underwood, M. C., Zhong, D., Mathur, A., Heyduk, T., and Bajaj, S. P. (2000) *J. Biol. Chem.* **275,** 36876–36884
10. Brandstetter, H., Kuhne, A., Bode, W., Huber, R., von der Saal, W., Wirthensohn, K., and Engh, R. A. (1996) *J. Biol. Chem.* **271,** 29988–29992
11. Zhang, E., and Tulinsky, A. (1997) *Biophys. Chem.* **63,** 185–200
12. Bode, W., and Schwager, P. (1975) *FEBS Lett.* **56,** 139–143
13. Wells, C. M., and Di Cera, E. (1992) *Biochemistry* **31,** 11721–11730
14. Di Cera, E., Guinto E. R., Vindigni, A., Dang, Q. D., Ayala, Y. M., Wuyi, M., and Tulinsky, A. (1995) *J. Biol. Chem.* **270,** 22089–22092
15. Dang, Q. D., and Di Cera, E. (1996) *Proc. Natl. Acad. Sci. U. S. A.* **93,** 10653–10656
16. De Cristofaro, R., Picozzi, M., Morosetti, R., and Landolfi, R. (1996) *J. Mol. Biol.* **258,** 190–200
17. De Cristofaro, R., and Landolfi, R. (1999) *Eur. J. Biochem.* **260,** 97–102
18. Rezaie, A. R., and He, X. (2000) *Biochemistry* **39,** 1817–1825
19. Schmidt, A. E., Padmanabhan, K., Underwood, M. C., Bode, W., Mather, T., and Bajaj, S. P. (2002) *J. Biol. Chem.* **277,** 28987–28995
20. Dang, Q. D., Vindigni, A., and Di Cera, E. (1995) *Proc. Natl. Acad. Sci. U. S. A.* **92,** 5977–5981
21. Monnaie, D., Arosio, D., Griffon, N., Rose, T., Rezaie, A. R., and Di Cera, E. (2000) *Biochemistry* **39,** 5349–5354
22. Guinto E. R., Caccia, S., Rose, T., Futterer, K., Waksman, G., and Di Cera, E. (1999) *Proc. Natl. Acad. Sci. U. S. A.* **96,** 1852–1857
23. Jordan, S. P., Mao, S. S., Lewis, S. D., and Shafer, J. A. (1992) *Biochemistry* **31,** 5374–5385
24. Evans, S. A., Olson, S. T., and Shore, J. D. (1982) *J. Biol. Chem.* **257,** 3014–3017
25. Lottenberg, R., and Jackson, C. M. (1983) *Biochim. Biophys. Acta* **742,** 558–564
26. Kim, D. J., and James, H. L. (1994) *Biotechnol. Lett.* **16,** 549–554
27. Barenholz, Y., Gibbes, D., Litman, B. J., Goll, J., Thompson, T. E., and Carlson, F. D. (1977) *Biochemistry* **16,** 2806–2810
28. Gomori, G. (1942) *J. Lab. Clin. Med.* **27,** 955–960
29. Krishnaswamy, S., Field, K. A., Edgington, T. S., Morrissey, J. H., and Mann, K. G. (1992) *J. Biol. Chem.* **267,** 26110–26120
30. Kisiel, W., Hermodson, M. A., and Davie, E. W. (1976) *Biochemistry* **15,** 4901–4906
31. Katzmann, J. A., Nesheim, M. E., Hibbard, L. S., and Mann, K. G. (1981) *Proc. Natl. Acad. Sci. U. S. A.* **78,** 162–166
32. Kalafatis, M., Krishnaswamy, S., Rand, M. D., and Mann, K. G. (1993) *Methods Enzymol.* **222,** 224–236
33. Gowda, D. C., Jackson, C. M., and Davidson, E. A. (1994) *J. Biol. Chem.* **269,** 10644–10650
34. Nordenman, B., Nystrom, C., and Björk, I. (1977) *Eur. J. Biochem.* **15,** 195–203
35. Mann, K. G. (1976) *Methods Enzymol.* **45,** 123–156
36. Lundblad, R. L., Kingdon, H. S., and Mann, K. G. (1976) *Methods Enzymol.* **45,** 156–176
37. Krishnaswamy, S., and Mann, K. G. (1988) *J. Biol. Chem.* **263,** 5714–5723
38. Di Scipio, R. G., Hermodson, M. A., Yates, S. G., and Davie, E. W. (1977) *Biochemistry* **16,** 698–706
39. Larson, P. J., Camire, R. M., Wong, D., Fasano, N. C., Monroe, D. M., Tracy, P. B., and High, K. A. (1998) *Biochemistry* **37,** 5029–5038
40. Camire, R. M., Larson, P. J., Stafford, D. W., and High, K. A. (2000) *Biochemistry* **39,** 14322–14329
41. Krishnaswamy, S., Church, W. R., Nesheim, M. E., and Mann, K. G. (1987) *J. Biol. Chem.* **262,** 3291–3299
42. Price, P. A. (1983) *Methods Enzymol.* **91,** 13–17
43. Przysiecki, C. T., Staggers, J. E., Ramjit, H. G., Musson, D. G., Stern, A. M., Bennett, C. D., and Friedman, P. A. (1987) *Proc. Natl. Acad. Sci. U. S. A.* **84,** 7856–7860
44. Krishnaswamy, S., and Betz, A. (1997) *Biochemistry* **36,** 12080–12086
45. Betz, A., Vlasuk, G. P., Bergum, P. W., and Krishnaswamy, S. (1997) *Biochemistry* **36,** 181–191
46. Krishnaswamy, S., Vlasuk, G. P., and Bergum, P. W. (1994) *Biochemistry* **33,** 7897–7907
47. Krishnaswamy, S., and Walker, R. K. (1997) *Biochemistry* **36,** 3319–3330
48. Bevington, P. R., and Robinson, K. D. (1992) *Data Reduction and Error Analysis for the Physical Sciences*, McGraw-Hill, New York
49. Straume, M., and Johnson, M. L. (1992) *Methods Enzymol.* **210,** 87–105
50. Segal, I. H. (1975) *Enzyme Kinetics: Behavior and Analysis of Rapid Equilibrium and Steady State Enzyme Systems*, John Wiley & Sons, Inc., New York
51. Lakowicz, J. R. (1983) *Principles of Fluorescence Spectroscopy*, Plenum Press, New York
52. Krishnaswamy, S. (1990) *J. Biol. Chem.* **265,** 3708–3718
53. Kuzmic, P. (1996) *Anal. Biochem.* **237,** 260–273
54. Stark, G. R., Stein, W. H., and Moore, S. (1960) *J. Biol. Chem.* **235,** 3177–3181
55. Plapp, B. V., Moore, S., and Stein, W. H. (1971) *J. Biol. Chem.* **246,** 939–945
56. Higashi, S., Matsumoto, N., and Iwanaga, S. (1996) *J. Biol. Chem.* **271,** 26569–26574
57. Petrovan, R. J., and Ruf, W. (2000) *Biochemistry* **39,** 14457–14463
58. Fehlhammer, H., Bode, W., and Huber, R. (1977) *J. Mol. Biol.* **111,** 415–438
59. Freer, S. T., Kraut, J., Robertus, J. D., Wright, H. T., and Xuong, N. H. (1970) *Biochemistry* **9,** 1997–2009
60. Huber, R., and Bode, W. (1978) *Acc. Chem. Res.* **11,** 114–122
61. Bode, W., Schwager, P., and Huber, R. (1978) *J. Mol. Biol.* **118,** 99–112
62. Venkateswarlu, D., Perera, L., Darden, T., and Pedersen, L. G. (2002) *Biophys. J.* **82,** 1190–1206
63. Griffon, N., and Di Stasio, E. (2001) *Biophys. Chem.* **90,** 89–96
64. Vijayalakshmi, J., Padmanabhan, K. P., Mann, K. G., and Tulinsky, A. (1994) *Protein Sci.* **3,** 2254–2271
65. Eigenbrot, C., Kirchhofer, D., Dennis, M. S., Santell, L., Lazarus, R. A., Stamos, J., and Ultsch, M. H. (2001) *Structure* **9,** 627–636
66. Nesheim, M. E., Eid, S., and Mann, K. G. (1981) *J. Biol. Chem.* **29,** 9874–9882
67. Walker, R. K., and Krishnaswamy, S. (1993) *J. Biol. Chem.* **268,** 13920–13929
68. Rudolph, A. E., Porche-Sorbet, R., and Miletich, J. P. (2000) *Biochemistry* **39,** 2861–2867
69. Bode, W., Mayr, I., Bauman, Y., Huber, R., Stone, S. R., and Hofsteenge, J. (1989) *EMBO J.* **8,** 3467–3475
70. Camire, R. M. (2000) *Blood* **96,** Abstr. 1929, 448a